arXiv:cond-mat/0601173v2 [cond-mat.supr-con] 9 Jan 2006

Dynamical spin susceptibility and the resonance peak in the pseudogap region of the underdoped cuprate superconductors

J.-P. Ismer[1,2], I. Eremin[2,3], Dirk K. Morr[1,4]
[1] *Institut für Theoretische Physik, Freie Universität Berlin, D-14195, Berlin, Germany*
[2] *Max-Planck Institut für Physik komplexer Systeme, D-01187 Dresden, Germany*
[3] *Institut für Mathematische/Theoretische Physik, Technische Universität Carolo-Wilhelmina zu Braunschweig, 38106 Braunschweig, Germany*
[4] *Department of Physics, University of Illinois at Chicago, Chicago, IL 60607*
(Dated: February 6, 2008)

We present a study of the dynamical spin susceptibility in the pseudogap region of the high-T_c cuprate superconductors. We analyze and compare the formation of the so-called resonance peak, in three different ordered states: the $d_{x^2-y^2}$-wave superconducting (DSC) phase, the d-density wave (DDW) state, and a phase with coexisting DDW and DSC order. An analysis of the resonance's frequency and momentum dependence in all three states reveals significant differences between them. In particular, in the DDW state, we find that a nearly dispersionless resonance excitation exists only in a narrow region around $\mathbf{Q} = (\pi, \pi)$. At the same time, in the coexisting DDW and DSC state, the dispersion of the resonance peak near $\mathbf{Q}$ is significantly changed from that in the pure DSC state. Away from (π, π), however, we find that the form and dispersion of the resonance excitation in the coexisting DDW and DSC state and pure DSC state are quite similar. Our results demonstrate that a detailed experimental measurement of the resonance's dispersion allows one to distinguish between the underlying phases - a DDW state, a DSC state, or a coexisting DDW and DSC state - in which the resonance peak emerges.

PACS numbers: 71.10.Ca,74.20.Fg,74.25.Ha,74.72.-h

I. INTRODUCTION

One of the most controversial topics in the field of high-temperature superconductivity is the origin of the so-called 'pseudogap' phenomenon observed by various experimental techniques in the underdoped cuprates (for a review see Ref.[1] and references therein). A large number of theoretical scenarios have been proposed to explain the origin of the pseudogap[2,3]. Among these is the d-density wave (DDW) scenario[3] which was suggested to explain some of the salient features of the underdoped cuprates such as the $d_{x^2-y^2}$-wave symmetry of the pseudogap above T_c, the anomalous behavior of the superfluid density[4] and of the Hall number[5], as well as the presence of weak (orbital) antiferromagnetism[6]. The DDW-phase is characterized by circulating bond currents which alternate in space, break time-reversal symmetry and result in an orbital (antiferromagnetically ordered) magnetic moment.

In this article, we investigate the momentum and frequency dependence of the dynamical spin susceptibility, $\chi(\mathbf{q}, \omega)$, in the underdoped region of the cuprate superconductors. In particular, we compare the formation of a resonant spin excitation (the "resonance peak") in three different ordered states: the DDW phase, the $d_{x^2-y^2}$-wave superconducting (DSC) phase, and a phase with coexisting DDW and DSC order. The observation of the resonance peak in inelastic neutron scattering (INS) experiments[7,8,9,10,11,12,13,14,15] is one of the key experimental facts in the phenomenology of the high-T_c cuprates. In the optimally and overdoped cuprates, the resonance peak appears below T_c in the dynamical spin susceptibility at the antiferromagnetic wave vector $\mathbf{Q} = (\pi, \pi)$. In the optimally doped cuprates, the resonance's frequency is $\omega_{res} \approx 41$ meV[7,11], a frequency which decreases with increasing underdoping[12,13]. A number of theoretical scenarios have been suggested for the appearance of the resonance peak in a superconducting state with $d_{x^2-y^2}$-wave symmetry[16,17,18]. In one of them, the so-called 'spin exciton' scenario[16,17], the resonance peak is attributed to the formation of a particle-hole bound state below the spin gap (a spin exciton), which is made possible by the specific momentum dependence of the $d_{x^2-y^2}$-wave gap. Within this scenario, the structure of spin excitations in the superconducting state as a function of momentum and frequency can be directly related to the topology of the Fermi surface and the phase of the superconducting order parameter. This scenario agrees well with the experimental data in the superconducting state of the optimally and overdoped cuprates. In the underdoped cuprates the resonance-like peak has also been observed in the pseudogap region above T_c as well as in the superconducting state[12,13,14,15]. In this article, we address the question whether in the underdoped cuprates, the resonance peak above T_c emerges from the presence of a DDW state, as first suggested by Tewari *et al.*[4], and below T_c from the coexistence of a DSC and DDW phase. To answer this question, we develop a spin exciton scenario for the pure DDW-phase as well as the coexisting DSC and DDW phases. By studying the detailed momentum and frequency dependence of the resonance peak in both phases, and by comparing it with that in the pure DSC state, we identify several characteristic features of the resonance peak that allow one to distinguish between the underlying phases, in which the

resonance peak emerges.

The remainder of the paper is organized as follows: in Secs. II and III we discuss the form of the resonance peak in the pure DDW phase and the coexisting DDW and DSC phase, respectively, and compare it with that in the pure DSC state. In Sec. IV we summarize our results and conclusions.

II. PURE DDW STATE

Starting point for our calculations in the pure DDW-state is the effective mean field Hamiltonian

$$H_{DDW} = \sum_{\mathbf{k},\sigma} \varepsilon_{\mathbf{k}} c^{\dagger}_{\mathbf{k},\sigma} c_{\mathbf{k},\sigma} + \sum_{\mathbf{k},\sigma} i W_{\mathbf{k}} c^{\dagger}_{\mathbf{k},\sigma} c_{\mathbf{k}+\mathbf{Q},\sigma} \qquad (1)$$

where $\mathbf{Q} = (\pi, \pi)$ is the ordering wavevector of the DDW state, $W_{\mathbf{k}} = \frac{W_0}{2}(\cos k_x - \cos k_y)$ is the DDW order parameter,

$$\varepsilon_{\mathbf{k}} = -2t\,(\cos k_x + \cos k_y) - 4t' \cos k_x \cos k_y - \mu \qquad (2)$$

is the normal state tight-binding energy dispersion with t, t' being the hopping elements between nearest and next-nearest neighbors, respectively, and μ is the chemical potential. In the following we use $t = 250$meV, $t'/t = -0.4$ and $\mu = -1.083t$. The Fermi surface (FS) obtained from Eq. (2) describes well the FS measured by photoemission experiments on $Bi_2Sr_2CaCu_2O_{8+\delta}$[19]. In order to directly compare the dynamical spin susceptibility in the DDW state with that in the DSC state, we take the DDW order parameter, $W_0 = 42$meV, to be equal to that in the DSC state[17]. We note here, that the above Hamiltonian can be obtained from a microscopic Hamiltonian with short-range repulsion or superexchange interactions[20,21]. After diagonalizing the Hamiltonian, Eq.(1), one finds that the excitation spectrum possesses two bands with energy dispersion

$$E^{\pm}_{\mathbf{k}} = \varepsilon^{+}_{\mathbf{k}} \pm \sqrt{\left(\varepsilon^{-}_{\mathbf{k}}\right)^2 + W^2_{\mathbf{k}}}\,, \qquad (3)$$

where $\varepsilon^{\pm}_{\mathbf{k}} = (\varepsilon_{\mathbf{k}} \pm \varepsilon_{\mathbf{k}+\mathbf{Q}})/2$. In Fig.1(a) we present the resulting Fermi surface in the DDW phase. Due to the doubling of the unit cell in the DDW state, the Fermi surface consists of hole pockets centered around $(\pm\pi/2, \pm\pi/2)$ and electron pockets around $(\pm\pi, 0)$ and $(0, \pm\pi)$. This type of Fermi surface has not yet been observed experimentally in the underdoped cuprates, possibly, as has recently been argued, due to additional interactions between quasiparticles[22]. For the above band parameters, the chemical potential lies within both branches of the excitation spectrum thus preventing the formation of a gap at the Fermi level. This is clearly visible from Fig.1(b) where we plot the density of states (DOS) for various values of the DDW gap. In particular, one finds that for $|t'| > W_0/4$ a suppression of (i.e., dip in) the DOS is formed away from the Fermi level which increases with

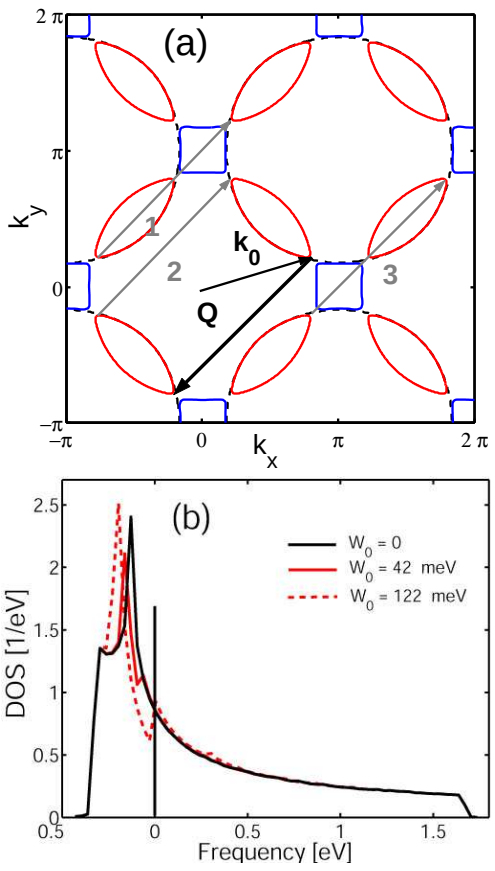

FIG. 1: (color online) (a) Fermi surface in the DDW state for $t = 250$meV, $t'/t = -0.4$, $\mu = -1.083t$ and $W_0 = 42$meV. The black and gray arrows represent the magnetic scattering vectors for $\mathbf{Q} = (\pi, \pi)$ and $\mathbf{Q}_i = 0.98(\pi, \pi)$, respectively. (b) Calculated DOS for several values of the DDW gap.

increasing W_0. In contrast, for $|t'| < W_0/4$, this suppression, which we identify with the pseudogap, opens at the Fermi level as was noted previously[23]. Note that for $t' = 0$, the DOS vanishes at the Fermi level, and the DOS resembles that of a $d_{x^2-y^2}$-wave superconductor.

In order to compute the dynamical spin susceptibility in the DDW state, we first introduce the spinor

$$\Psi^{\dagger}_{\mathbf{k},\sigma} = \left(c^{\dagger}_{\mathbf{k},\sigma}, c^{\dagger}_{\mathbf{k}+\mathbf{Q},\sigma}\right)\,, \qquad (4)$$

where σ is the spin index, and the electronic Greens function in the DDW state is defined as $\hat{G}_{\sigma}(\mathbf{k}, \tau - \tau') = -\langle \mathcal{T} \Psi_{\mathbf{k},\sigma}(\tau) \Psi^{\dagger}_{\mathbf{k},\sigma}(\tau') \rangle$. The bare (non-interacting) part of the dynamical spin susceptibility per spin degree of freedom is then given by

$$\chi_0(\mathbf{q}, i\Omega_m) = -\frac{T}{8} {\sum_{\mathbf{k},n}}' \mathrm{Tr}\left[\hat{G}(\mathbf{k}, i\omega_n) \times \hat{G}(\mathbf{k}+\mathbf{q}, i\omega_n - i\Omega_m)\right] \qquad (5)$$

where $\hat{G}(\mathbf{k}, i\omega_n) = \hat{G}_{\sigma}(\mathbf{k}, i\omega_n)\hat{\sigma}_0$ is the Green's function

matrix in momentum and Matsubara space[24], and the primed sum runs over the reduced fermionic Brillouin zone of the DDW state. Note that with the above definition, one has $\chi_0^{zz} = 2\chi_0$. After performing the summation over the internal Matsubara frequencies and analytic continuation to the real frequency axis, one obtains for the retarded spin susceptibility in the DDW phase

$$\chi_0(\mathbf{q},\omega) = \frac{1}{8}\sum_{\mathbf{k}}{}' \left(1 + \frac{\varepsilon^-_{\mathbf{k}}\varepsilon^-_{\mathbf{k+q}} + W_{\mathbf{k}}W_{\mathbf{k+q}}}{\sqrt{\left(\varepsilon^-_{\mathbf{k}}\right)^2 + W^2_{\mathbf{k}}}\sqrt{\left(\varepsilon^-_{\mathbf{k+q}}\right)^2 + W^2_{\mathbf{k+q}}}}\right)\left(\frac{f(E^+_{\mathbf{k+q}}) - f(E^+_{\mathbf{k}})}{\omega + i0^+ - E^+_{\mathbf{k+q}} + E^+_{\mathbf{k}}} + \frac{f(E^-_{\mathbf{k+q}}) - f(E^-_{\mathbf{k}})}{\omega + i0^+ - E^-_{\mathbf{k+q}} + E^-_{\mathbf{k}}}\right)$$
$$+ \left(1 - \frac{\varepsilon^-_{\mathbf{k}}\varepsilon^-_{\mathbf{k+q}} + W_{\mathbf{k}}W_{\mathbf{k+q}}}{\sqrt{\left(\varepsilon^-_{\mathbf{k}}\right)^2 + W^2_{\mathbf{k}}}\sqrt{\left(\varepsilon^-_{\mathbf{k+q}}\right)^2 + W^2_{\mathbf{k+q}}}}\right)\left(\frac{f(E^-_{\mathbf{k+q}}) - f(E^+_{\mathbf{k}})}{\omega + i0^+ - E^-_{\mathbf{k+q}} + E^+_{\mathbf{k}}} + \frac{f(E^+_{\mathbf{k+q}}) - f(E^-_{\mathbf{k}})}{\omega + i0^+ - E^+_{\mathbf{k+q}} + E^-_{\mathbf{k}}}\right) \quad (6)$$

where $f(\epsilon)$ is the Fermi function.

We first analyze the behavior of the imaginary part of χ_0 at $\mathbf{Q} = (\pi,\pi)$, and present in Fig. 2 $\mathrm{Im}\chi_0(\mathbf{Q},\omega)$ as a function of frequency in the normal state, the DSC state, and the DDW state[25] (for the form of χ_0 in the DSC state, see Ref.[17]). The behavior of $\mathrm{Im}\chi_0(\mathbf{Q},\omega)$ in the normal and DSC state have been extensively discussed in the literature (see, for example, Ref.[16,17,18]). In the normal state $\mathrm{Im}\chi_0$ increases linearly at low frequencies with a slope determined by the Landau damping rate, while, at higher energies its behavior is determined by the presence of the van Hove singularity. In contrast, in the superconducting state the susceptibility is gapped up to an energy $\Omega_{cr}^{DSC} = \min_{\mathbf{k}}\left(|\Delta_{\mathbf{k}}| + |\Delta_{\mathbf{k+Q}}|\right)$ where $\Delta_{\mathbf{k}}$ is the superconducting gap and both $\mathbf{k}$ and $\mathbf{k}+\mathbf{Q}$ lie on the Fermi surface. Due to the symmetry of the superconducting gap, one finds $\Delta_{\mathbf{k}} = -\Delta_{\mathbf{k+Q}}$, resulting in a discontinuous jump of $\mathrm{Im}\chi_0$ at Ω_{cr}^{DSC}[16,17].

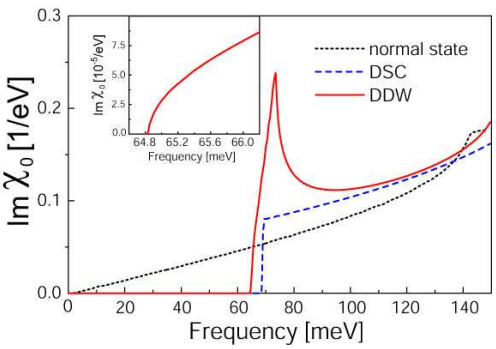

FIG. 2: (color online) Imaginary part of $\chi_0(\mathbf{Q},\omega)$ at $\mathbf{Q} = (\pi,\pi)$ in the normal, DSC, and DDW state as a function of frequency. The momentum dependence of the superconducting gap is taken to be $\Delta(k) = \Delta_0(\cos k_x - \cos k_y)/2$, with $\Delta_0 = W_0 = 42$meV. Inset: $\mathrm{Im}\chi_0(\mathbf{Q},\omega)$ in the DDW phase as a function of frequency around Ω_{cr}^{DDW}.

In order to discuss the behavior of $\mathrm{Im}\chi_0$ in the DDW-state, we first note that the expression for χ_0 in Eq.(6) contains two terms that describe intraband scattering within the $E^{\pm}_{\mathbf{k}}$-bands, and two terms that represent interband scattering between the two bands. Since $E^{\pm}_{\mathbf{k+Q}} = E^{\pm}_{\mathbf{k}}$ the intraband scattering terms do not contribute to $\mathrm{Im}\chi_0$ at $\mathbf{Q}$. Moreover, since $E^-_{\mathbf{k}} \leq E^+_{\mathbf{k}}$ the first interband scattering term yields a non-zero contribution to $\mathrm{Im}\chi_0$ only for negative frequencies. Thus, only the second interband scattering term in Eq.(6) contributes to $\mathrm{Im}\chi_0$ at $\mathbf{Q}$. Since the Fermi surfaces of the two energy bands, $E^{\pm}_{\mathbf{k}}$, cannot be connected by the wave vector $\mathbf{Q}$, as is evident from Fig.1(a), $\mathrm{Im}\chi_0$ is gapped at low frequencies up to an energy $\Omega_{cr}^{DDW} \approx 64.8$ meV. The latter is determined by the minimum value of $E^+_{\mathbf{k}} - E^-_{\mathbf{k}} = 2\sqrt{\left(\varepsilon^-_{\mathbf{k}}\right)^2 + W^2_{\mathbf{k}}}$ in the DDW Brillouin zone, a condition that is set by the δ-function arising from the last term in Eq.(6) for $\mathrm{Im}\chi_0$. Note that $\varepsilon^-_{\mathbf{k}} \equiv 0$ along the boundary of the DDW Brillouin zone. Due to the requirement $sgn(E^+_{\mathbf{k}}) \neq sgn(E^-_{\mathbf{k}})$, we find that $\Omega_{cr}^{DDW} = 2|W_{\mathbf{k_0}}|$ where $\mathbf{k_0}$ is the momentum at which the hole pocket around $(\pi/2,\pi/2)$ is intersected by the DDW Brillouin zone boundary (see Fig. 1). Moreover, since $\varepsilon^-_{\mathbf{k+Q}} = -\varepsilon^-_{\mathbf{k}}$ and $W_{\mathbf{k+Q}} = -W_{\mathbf{k}}$, the second coherence factor in Eq.(6) is identical to 2 for all momenta. Note that there exist two important differences in $\mathrm{Im}\chi_0$ between the DDW and DSC state. First, in the DSC state, $\mathrm{Im}\chi_0 \neq 0$ requires that the frequency exceeds $\Omega_{cr}^{DSC} = \min_{\mathbf{k}}\left(|\Delta_{\mathbf{k}}| + |\Delta_{\mathbf{k+Q}}|\right)$, a condition which is set by the δ-function in $\mathrm{Im}\chi_0$ (see Eq.(6)) and simply reflects energy conservation. In contrast, in the DDW-state, $\mathrm{Im}\chi_0 \neq 0$ requires (a) that $\omega - E^+_{\mathbf{k+Q}} + E^-_{\mathbf{k}} = 0$ for certain momenta $\mathbf{k}$, and (b) that for the same momenta $f(E^+_{\mathbf{k+q}}) - f(E^-_{\mathbf{k}}) \neq 0$. We find that there exist momenta for which (a) is satisfied at frequencies $\omega < \Omega_{cr}^{DDW}$, but that for the same momenta $f(E^+_{\mathbf{k+q}}) - f(E^-_{\mathbf{k}}) = 0$ (at $T = 0$). In other words, the critical frequency Ω_{cr}^{DDW} for the onset of a non-zero $\mathrm{Im}\chi_0$ is determined by the difference in the population of the states that are in-

volved in the scattering process, and not by energy conservation as in the superconducting state. This qualitative difference between the DDW and the DSC state bears important consequences: for $\omega > \Omega_{cr}^{DDW}$, one has $\mathrm{Im}\chi_0 \sim \sqrt{\omega - \Omega_{cr}^{DDW}}$, in contrast to the discontinuous jump of $\mathrm{Im}\chi_0$ at Ω_{cr}^{DSC} in the DSC state (this result for the DDW state differs from that in Ref.[4] due to the different Fermi surface topology considered here). This behavior becomes immediately apparent when one plots $\mathrm{Im}\chi_0$ in the DDW-state around $\omega = \Omega_{cr}^{DDW}$, as shown in the inset of Fig. 2. Note that the number of momenta which are involved in scattering processes and thus contribute to $\mathrm{Im}\chi_0$ rapidly increases for $\omega > \Omega_{cr}^{DDW}$ due to a steeply increasing density of states of the function $E_{\mathbf{k}}^{+} - E_{\mathbf{k}}^{-} = 2\sqrt{\left(\varepsilon_{\mathbf{k}}^{-}\right)^2 + W_{\mathbf{k}}^2}$, which gives rise to the peak in $\mathrm{Im}\chi_0$ at $\omega_p \approx 73$ meV.

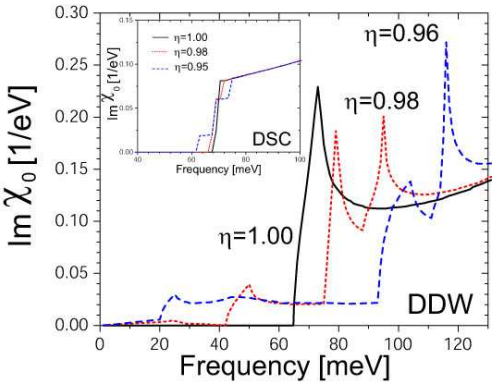

FIG. 3: (color online) $\mathrm{Im}\chi_0$ in the DDW state as a function of frequency for several momenta $\mathbf{q} = \eta(\pi, \pi)$ along the diagonal of the magnetic Brillouin zone (BZ). Inset: $\mathrm{Im}\chi_0$ in the DSC state as a function of frequency for several momenta $\mathbf{q} = \eta(\pi, \pi)$.

For momenta $\mathbf{q} \neq \mathbf{Q}$, the behavior of $\mathrm{Im}\chi_0$ in the DDW state is more complex, since in addition to interband scattering, intraband scattering is now possible. In Fig. 3, we plot the frequency dependence of $\mathrm{Im}\chi_0$ for several momenta in the DDW state (for comparison, $\mathrm{Im}\chi_0$ in the DSC state is shown in the inset). We find that as one moves away from $\mathbf{Q} = (\pi, \pi)$, several square-root-like increases in $\mathrm{Im}\chi_0$ appear, with the one lowest in energy rapidly decreasing in frequency. In order to better understand the combined frequency and momentum dependence of $\mathrm{Im}\chi_0$ in the DDW state, we present in Fig. 4 the contributions to $\mathrm{Im}\chi_0$ at $\mathbf{Q}_i = 0.98\mathbf{Q}$ from interband scattering [Fig. 4(a)] and intraband scattering within the E_k^{+}-band [Fig. 4(b)] and E_k^{-}-band [Fig. 4(c)] separately. Note that while the contribution from intraband scattering is approximately two orders of magnitude smaller than that from interband scattering, the former continuously increases from zero energy, such that $\mathrm{Im}\chi_0$ does not any longer exhibit a gap. This result is valid for all momenta $\mathbf{q} \neq \mathbf{Q}$ in the vicinity of $\mathbf{Q}$. In contrast, the interband scattering term possesses three critical frequencies, $\Omega_{cr}^{(i)} (i = 1, 2, 3)$, which arise from the opening of three non-degenerate scattering channels that are described by the scattering momenta shown in Fig. 1(a). These three critical energies are indicated by arrows in Fig. 4(a). For all three scattering channels, the coherence factor is approximately 2. Note that the first and third scattering channel, which open at $\Omega_{cr}^{(1)} \approx 43$ meV and $\Omega_{cr}^{(3)} \approx 88$ meV and are described by arrow (1) and (3) in Fig. 1(a), respectively, connect momenta $\mathbf{k}$ and $\mathbf{k}'$ with $\mathbf{k} - \mathbf{k}' = \mathbf{Q}_i - (\pi, \pi)$ and thus represent umklapp scattering. In contrast, channel (2) which opens at $\Omega_{cr}^{(2)} \approx 76$ meV [see arrow (2) in Fig. 1(a)] describes direct scattering with $\mathbf{k} - \mathbf{k}' = \mathbf{Q}_i$. The opening of each of these three scattering channels is accompanied by a square-root like increase of $\mathrm{Im}\chi_0$. Note that the lowest threshold frequency for interband transitions vanishes at $\mathbf{Q}_i = 0.94\mathbf{Q}$, since this wave vector connects momenta on the Fermi surfaces of the $E_{\mathbf{k}}^{+}$ and $E_{\mathbf{k}}^{-}$ bands.

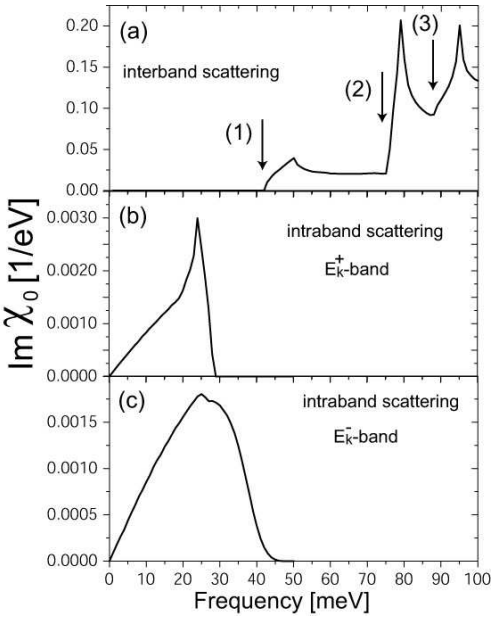

FIG. 4: Contributions to $\mathrm{Im}\chi_0$ at $\mathbf{Q}_i = 0.98\mathbf{Q}$ from (a) interband scattering, (b) interband scattering within the E_k^{+}-band, and (c) interband scattering within the E_k^{-}-band. The arrows in (a) indicate the critical frequencies for the opening of interband scattering channels. The transitions in the fermionic BZ corresponding to the opening of the interband scattering channels are shown in Fig.1(a).

The emergence of a resonance peak in the DDW state can be understood by considering the dynamical spin susceptibility within the random phase approximation (RPA). Within this approximation[27], the susceptibility (per spin degree of freedom) is given by

$$\chi_{RPA}(\mathbf{q}, \omega) = \frac{\chi_0(\mathbf{q}, \omega)}{1 - U\chi_0(\mathbf{q}, \omega)} \ , \qquad (7)$$

where U is the fermionic four-point vertex. We first con-

sider $\mathbf{q} = \mathbf{Q}$ and note that in the superconducting state, the discontinuous jump in $\mathrm{Im}\chi_0$ leads to logarithmic singularity in $\mathrm{Re}\chi_0$. As a result, the resonance conditions, $U\mathrm{Re}\chi_0(\mathbf{Q}, \omega = \omega_{res}) = 1$ and $\mathrm{Im}\chi_0(\mathbf{Q}, \omega = \omega_{res}) = 0$, can be fulfilled simultaneously below the particle-hole continuum for an arbitrarily small value of $U > 0$, leading to the emergence of a resonance peak as a spin exciton. In contrast, in the DDW state, $\mathrm{Im}\chi_0$ exhibits a square-root like frequency dependence above Ω_{cr}^{DDW}, leading to an increase of $\mathrm{Re}\chi_0$ at the critical frequency, but not to a singularity in $\mathrm{Re}\chi_0$. Specifically, we find

$$\mathrm{Re}\,\chi_0 = \frac{2\sqrt{W}}{\pi}\,\alpha\,\mathrm{Re}\left[2 - \sqrt{\frac{\Delta_-}{W}}\arctan\left(\sqrt{\frac{W}{\Delta_-}}\right) - \sqrt{\frac{\Delta_+}{W}}\arctan\left(\sqrt{\frac{W}{\Delta_+}}\right)\right] + ... \tag{8}$$

where $W = E_c - \Omega_{cr}^{DDW}$, E_c is the high energy cut-off for the square-root like frequency dependence of $\mathrm{Im}\chi_0 = \alpha\sqrt{\omega - \Omega_{cr}^{DDW}}$, $\Delta_\pm = \Omega_{cr}^{DDW} \pm \omega$ and the ellipsis denote background contributions to $\mathrm{Re}\chi_0$ that are independent of the opening of a new scattering channel. The above form of $\mathrm{Re}\chi_0$ implies that U now has to exceed a critical value, U_c, before a resonance peak (in the form of a spin exciton) can emerge in the DDW state. We note, however, that the values of U typically taken to describe the emergence of a resonance peak in the DSC state of optimally doped cuprate superconductors, exceed U_c, such that a resonance peak also emerges in the DDW state. In other words, for $U > U_c$, the resonance conditions $U\mathrm{Re}\chi_0(\mathbf{Q}, \omega = \omega_{res}) = 1$ and $\mathrm{Im}\chi_0(\mathbf{Q}, \omega = \omega_{res}) = 0$ are satisfied in the DDW state at a frequency $\omega_{res} < \Omega_{cr}^{DDW}$. As a result, a resonance peak emerges in the RPA spin susceptibility around $\mathbf{Q} = (\pi, \pi)$, as shown in Fig.5 (the value of U is chosen such that in the DSC state, $\omega_{res} = 41$ meV). Away from $\mathbf{Q}$, the mode becomes rapidly damped due to the opening of a scattering channel for intraband transitions, as discussed above. In addition, the lowest critical frequency for interband transitions rapidly decreases to zero. As a result, the resonance peak in the DDW state is confined to the immediate vicinity of $\mathbf{Q} = (\pi, \pi)$, and shows no significant dispersion. Note, that the upward and downward structures in $\mathrm{Im}\chi_{RPA}$ visible in Fig. 5 do not represent real poles in the susceptibility but arise from the frequency structure of $\mathrm{Im}\chi_0$ away from (π, π). This momentum dependence of the 'spin exciton' in the DDW state stands in stark contrast to the dispersion of the resonance peak in the DSC state[17] (see Fig. 9).

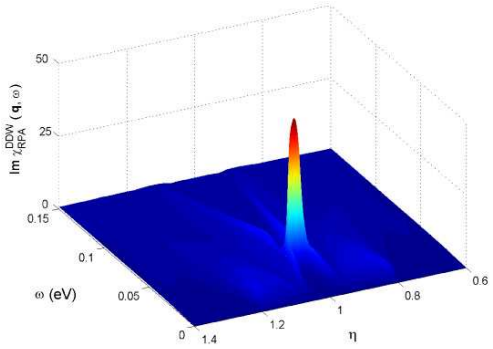

FIG. 5: (color online) Imaginary part of the RPA spin susceptibility in the DDW state as a function of frequency and momentum along the diagonal of the first BZ for $U = 2.24$eV.

III. COEXISTING DDW AND DSC PHASES

We next consider a state with coexisting DDW and DSC order whose mean-field Hamiltonian is given by

$$\mathcal{H}^{DSC+DDW} = \sum_k \psi_k^\dagger H(k)\psi_k \quad , \tag{9}$$

where $\psi_{\mathbf{k}}^\dagger = \left(c_{\mathbf{k}\uparrow}^\dagger, c_{\mathbf{k}+\mathbf{Q}\uparrow}^\dagger, c_{-\mathbf{k}\downarrow}, c_{-\mathbf{k}-\mathbf{Q}\downarrow}\right)$ and[4]

$$H_{\mathbf{k}} = \begin{pmatrix} \varepsilon_{\mathbf{k}} & iW_{\mathbf{k}} & \Delta_{\mathbf{k}} & 0 \\ -iW_{\mathbf{k}} & \varepsilon_{\mathbf{k}+\mathbf{Q}} & 0 & -\Delta_{\mathbf{k}} \\ \Delta_{\mathbf{k}} & 0 & -\varepsilon_k & iW_{\mathbf{k}} \\ 0 & -\Delta_{\mathbf{k}} & -iW_{\mathbf{k}} & -\varepsilon_{\mathbf{k}+\mathbf{Q}} \end{pmatrix} \quad . \tag{10}$$

The energy bands arising from diagonalizing the Hamiltonian in Eq.(10) are given by

$$\Omega_{\mathbf{k}}^\pm = \sqrt{\left(E_{\mathbf{k}}^\pm\right)^2 + \Delta_{\mathbf{k}}^2}\,, \tag{11}$$

with $E_{\mathbf{k}}^\pm$ being the energy bands of the pure DDW state given above. The bare susceptibility, χ_0 in the coexisting phase can again be calculated using Eq.(5) with the only difference that the Green's function $\hat{G}_\sigma(\mathbf{k}, i\omega_n)$ is now a (4×4) matrix. The full expression for χ_0 in the coexistence phase is somewhat lengthy and therefore given in Appendix A.

In Fig. 6 we present $\mathrm{Im}\chi_0$ as a function of frequency for several momenta $\mathbf{q} = \eta(\pi, \pi)$ along the diagonal of the magnetic BZ. At $\mathbf{Q} = (\pi, \pi)$ $(\eta = 1.0)$, $\mathrm{Im}\chi_0$ exhibits a single discontinuous jumps at the critical frequency, $\Omega_{cr}^{coex} = 97$ meV. The magnetic scattering asso-

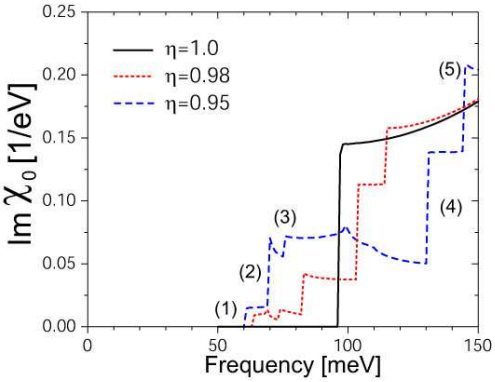

FIG. 6: (color online) Im χ_0 as a function of frequency in the coexisting DDW and DSC state for several momentum $\mathbf{q} = \eta(\pi, \pi)$ along the diagonal of the magnetic BZ.

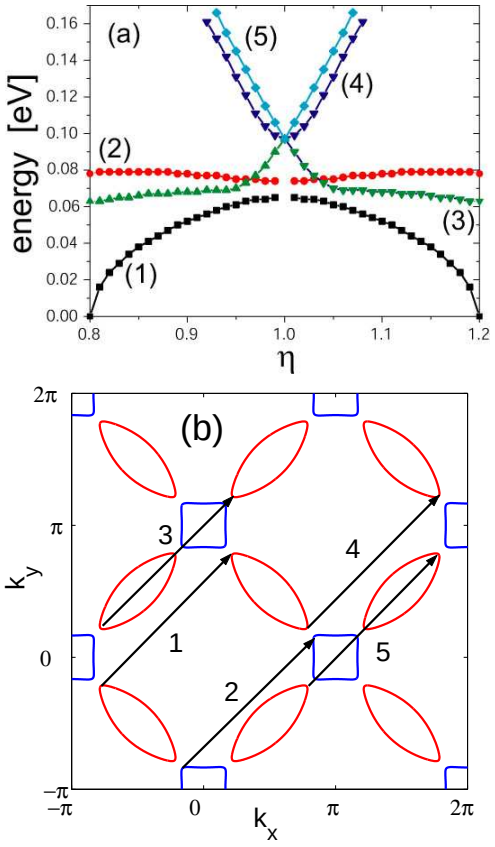

FIG. 7: (color online)(a) Momentum dependence of the critical frequencies $\Omega_{cr}^{(i)}$ $(i = 1, .., 5)$. (b) FS of the pure DDW state and magnetic scattering vectors of the 5 scattering channels that open at $\Omega_{cr}^{(i)}$.

ciated with the opening of this scattering channel connects the "hot spots" in the fermionic BZ, i.e., those momenta $\mathbf{k}$ and $\mathbf{k}+\mathbf{Q}$ for which $\varepsilon_{\mathbf{k}} = \varepsilon_{\mathbf{k}+\mathbf{Q}} = 0$. Correspondingly, the critical frequency is given by $\Omega_{cr}^{coex} = 2\sqrt{\Delta^2(\mathbf{k}_{hs}) + W^2(\mathbf{k}_{hs})}$ where $\mathbf{k}_{hs}$ is the momentum of the hot spots. In contrast, away from $\mathbf{Q} = (\pi, \pi)$, we find that Imχ_0 exhibits 5 discontinuous jumps at critical frequencies, $\Omega_{cr}^{(i)}$ with $i = 1, .., 5$ indicating the opening of new scattering channels (for $\eta = 0.95$ these five discontinuous jumps are labeled in Fig. 6). Note that in the coexistence phase, the opening of a new scattering channel is accompanied by a discontinuous jump, similar to the pure DSC state, but in contrast to the DDW state, as discussed above. The momentum dependence of these critical frequencies is shown in Fig. 7(a). At $\Omega_{cr}^{(1)}$ $[\Omega_{cr}^{(2)}]$, a scattering channel for intraband scattering within the $\Omega_{\mathbf{k}}^{+}$ $(\Omega_{\mathbf{k}}^{-})$ band opens, and Imχ_0 acquires a non-zero contribution from $\chi^{(2)}$ $(\chi^{(5)})$ given in Eq.(A3) [Eq.(A6)] of Appendix A. As follows directly from Eqs.(A3) and (A6), the coherence factors associated with these two scattering processes vanish identically at $\mathbf{Q} = (\pi, \pi)$, and hence, no value for $\Omega_{cr}^{(1,2)}$ can be defined at this momentum. However, away from $\mathbf{Q} = (\pi, \pi)$, the coherence factors are not longer zero, and two discontinuous jumps appear in Imχ_0 that are associated with the opening of two new scattering channels at $\Omega_{cr}^{(1,2)}$. Note that the magnitude of the jumps at $\Omega_{cr}^{(1,2)}$ increases as one moves away from $\mathbf{Q} = (\pi, \pi)$, which is a direct consequence of the increasing coherence factors. Similar to the superconducting state the lowest critical frequency, $\Omega_{cr}^{(1)}$, reaches zero at $\eta = 0.8(\pi, \pi)$. In contrast, at $\Omega_{cr}^{(3,4,5)}$ new scattering channels for interband scattering between the $\Omega_{\mathbf{k}}^{+}$ and $\Omega_{\mathbf{k}}^{-}$ bands are opened. These three critical frequencies are degenerate at $\mathbf{Q} = (\pi, \pi)$, but this degeneracy is lifted for $\mathbf{q} \neq \mathbf{Q}$, as follows immediately from Fig. 7(a). For $\eta = 0.98$, we present in Fig. 7(b) the scattering momenta that are associated with the opening of the above discussed five scattering channels. For completeness, we also present the Fermi surfaces for the $E_k^{\pm}$ bands. Note, that the scattering vectors (1) and (2) describe intraband scattering within the $\Omega_{\mathbf{k}}^{+}$ and $\Omega_{\mathbf{k}}^{-}$ bands, while the scattering vectors (3), (4) and (5) represent interband scattering. The scattering vectors (3), (4), and (5) are identical to those present in the pure DDW state [for comparison, see Fig.1 (a)].

In Fig. 8 we present the RPA susceptibility in the coexisting DDW and DSC phase. Similarly to the pure DSC state, the discontinuous jump in Imχ_0 in the coexistence phase is accompanied by a logarithmic divergence in Reχ_0, which in turn gives rise to a resonance peak below the particle-hole continuum for an arbitrary small fermionic interaction. A comparison with the RPA susceptibility in the pure DSC state shown in Fig. 8(b) reveals that the frequency position of the resonances peak varies more quickly with momentum (near $\mathbf{Q} = (\pi, \pi)$) in the coexistence phase than in the pure DSC state. This difference becomes particularly evident when one plots the dispersion of the resonance peak both in the coexistence phase and the pure DSC state, as shown in Fig. 9. We find that the difference in the dispersion of the resonance peaks is particularly pronounced around $\mathbf{Q}$ $(0.95 \lesssim \eta \lesssim 1.05)$, with a more cusp-like dispersion in the coexistence phase. This cusp follows the form of

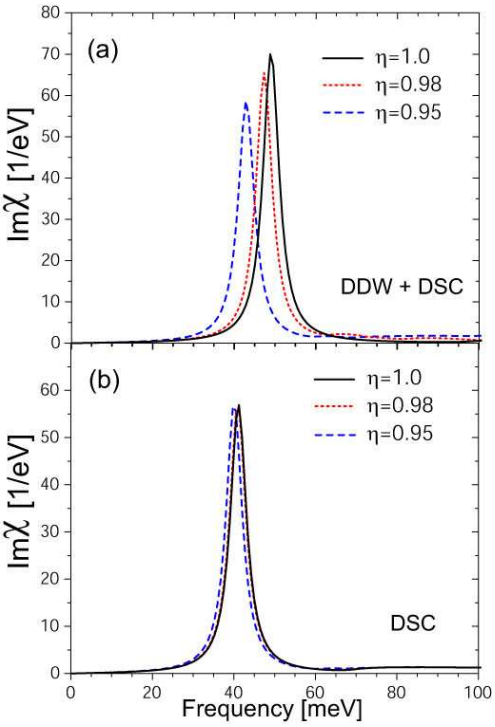

FIG. 8: (color online) (a) RPA spin susceptibility as a function of frequency in the coexisting DDW and DSC state for several momenta. (b) RPA spin susceptibility as a function of frequency in the pure DSC state for several momenta.

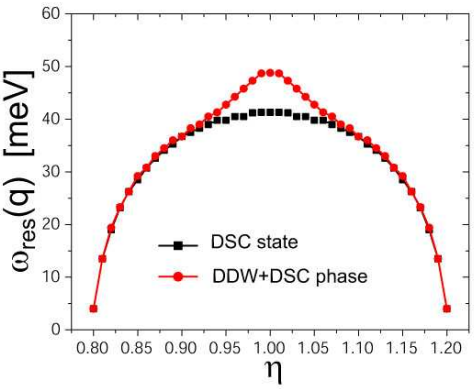

FIG. 9: (color online) Dispersion of the resonance peak in the coexisting DDW and DSC state, as well as in the pure DSC state.

the particle-hole continuum in the vicinity of **Q** in the coexistence phase, as is evident from Fig. 7(a). Thus the dispersion of the resonance peak directly reflects the different momentum dependence of the particle-hole continuum in the vicinity of **Q** in the coexisting DDW and DSC state and the pure DSC state. However, away from **Q**, the particle-hole continuum, as well as the dispersion of the resonance peak are quite similar in both phases.

IV. CONCLUSIONS

In conclusion, we have analyzed the momentum and frequency dependence of the dynamical spin susceptibility in the pure DDW state and the phase with coexisting DDW and DSC order. We find that due to the opening of a spin gap in $\mathrm{Im}\chi_0$ in both phases, a resonance peak emerges below the particle-hole continuum. However, in the DDW state, $\mathrm{Im}\chi_0$ exhibits a square-root like increase at the critical frequencies, in contrast to the coexisting DDW and DSC phases (or the pure DSC phase), where the onset of $\mathrm{Im}\chi_0 \neq 0$ is accompanied by a discontinuous jump. As a result, $\mathrm{Re}\chi_0$ in the DDW state does not exhibit a divergence, but simply an enhancement at the critical frequency, and hence, a finite fermionic interaction strength is necessary for the emergence of a resonance peak in the DDW state. This result is qualitatively different from the coexisting DDW and DSC phase and the pure DSC state where a resonance peak emerges for an infinitesimally small interaction strength. We note, however, that for the strength of the fermionic interaction usually taken to describe the resonance peak in the DSC state, a resonance peak also emerges in the DDW state. Moreover, we find that the resonance peak in the DDW state is basically dispersionless and confined to the vicinity of $\mathbf{Q} = (\pi, \pi)$ due to the form of the particle-hole continuum in the DDW state. In contrast, the dispersion of the resonance peak in the coexisting DDW and DSC state is similar to that in the pure DSC state, with the exception that in the vicinity of **Q**, the former exhibits a cusp. These results show that the detailed momentum and frequency dependence of the resonance peak is different in all three phases, the pure DDW, pure DSC and coexisting DDW and DSC phases. Thus, a detailed experimental study of the resonance peak in the underdoped cuprates permits one to identify the nature of the underlying phase in which the resonance peaks emerges. We believe, however, that the currently available experimental INS data do not yet allow an unambiguous conclusion with regards to the nature of the phases present in the underdoped cuprate superconductors.

D.K.M. acknowledges financial support by the Alexander von Humboldt Foundation, the National Science Foundation under Grant No. DMR-0513415 and the U.S. Department of Energy under Award No. DE-FG02-05ER46225.

APPENDIX A: DYNAMICAL SPIN SUSCEPTIBILITY IN THE REGIME OF COEXISTING DDW+DSC PHASES

In the coexisting DDW and d-wave superconducting phase, the susceptibility is given by

$$\chi(\mathbf{q},\omega)=\sum_i \chi^{(i)}(\mathbf{q},\omega) \tag{A1}$$

where

$$\chi^{(1)}(\mathbf{q},\omega) = \frac{1}{16}\sum_{\mathbf{k}}\left(1+\frac{E^+_{\mathbf{k}}E^+_{\mathbf{k+q}}+\Delta_{\mathbf{k}}\Delta_{\mathbf{k+q}}}{\Omega^+_{\mathbf{k}}\Omega^+_{\mathbf{k+q}}}\right)\left(1+\frac{\varepsilon^-_{\mathbf{k}}\varepsilon^-_{\mathbf{k+q}}+W_{\mathbf{k}}W_{\mathbf{k+q}}}{\sqrt{\left(\varepsilon^-_{\mathbf{k}}\right)^2+W^2_{\mathbf{k}}}\sqrt{\left(\varepsilon^-_{\mathbf{k+q}}\right)^2+W^2_{\mathbf{k+q}}}}\right)\frac{f(\Omega^+_{\mathbf{k+q}})-f(\Omega^+_{\mathbf{k}})}{\omega-\Omega^+_{\mathbf{k+q}}+\Omega^+_{\mathbf{k}}+i\delta} \tag{A2}$$

$$\begin{aligned}\chi^{(2)}(\mathbf{q},\omega) &= \frac{1}{32}\sum_{\mathbf{k}}\left(1-\frac{E^+_{\mathbf{k}}E^+_{\mathbf{k+q}}+\Delta_{\mathbf{k}}\Delta_{\mathbf{k+q}}}{\Omega^+_{\mathbf{k}}\Omega^+_{\mathbf{k+q}}}\right)\left(1+\frac{\varepsilon^-_{\mathbf{k}}\varepsilon^-_{\mathbf{k+q}}+W_{\mathbf{k}}W_{\mathbf{k+q}}}{\sqrt{\left(\varepsilon^-_{\mathbf{k}}\right)^2+W^2_{\mathbf{k}}}\sqrt{\left(\varepsilon^-_{\mathbf{k+q}}\right)^2+W^2_{\mathbf{k+q}}}}\right)\\ &\times\left(\frac{1-f(\Omega^+_{\mathbf{k+q}})-f(\Omega^+_{\mathbf{k}})}{\omega+\Omega^+_{\mathbf{k+q}}+\Omega^+_{\mathbf{k}}+i\delta}+\frac{f(\Omega^+_{\mathbf{k+q}})+f(\Omega^+_{\mathbf{k}})-1}{\omega-\Omega^+_{\mathbf{k+q}}-\Omega^+_{\mathbf{k}}+i\delta}\right)\end{aligned} \tag{A3}$$

$$\begin{aligned}\chi^{(3)}(\mathbf{q},\omega) &= \frac{1}{16}\sum_{\mathbf{k}}\left(1+\frac{E^+_{\mathbf{k}}E^-_{\mathbf{k+q}}+\Delta_{\mathbf{k}}\Delta_{\mathbf{k+q}}}{\Omega^+_{\mathbf{k}}\Omega^-_{\mathbf{k+q}}}\right)\left(1-\frac{\varepsilon^-_{\mathbf{k}}\varepsilon^-_{\mathbf{k+q}}+W_{\mathbf{k}}W_{\mathbf{k+q}}}{\sqrt{\left(\varepsilon^-_{\mathbf{k}}\right)^2+W^2_{\mathbf{k}}}\sqrt{\left(\varepsilon^-_{\mathbf{k+q}}\right)^2+W^2_{\mathbf{k+q}}}}\right)\\ &\times\left(\frac{f(\Omega^-_{\mathbf{k+q}})-f(\Omega^+_{\mathbf{k}})}{\omega-\Omega^-_{\mathbf{k+q}}+\Omega^+_{\mathbf{k}}+i\delta}+\frac{f(\Omega^+_{\mathbf{k}})-f(\Omega^-_{\mathbf{k+q}})}{\omega-\Omega^+_{\mathbf{k}}+\Omega^-_{\mathbf{k+q}}+i\delta}\right)\end{aligned} \tag{A4}$$

$$\begin{aligned}\chi^{(4)}(\mathbf{q},\omega) &= \frac{1}{16}\sum_{\mathbf{k}}\left(1-\frac{E^+_{\mathbf{k}}E^-_{\mathbf{k+q}}+\Delta_{\mathbf{k}}\Delta_{\mathbf{k+q}}}{\Omega^+_{\mathbf{k}}\Omega^-_{\mathbf{k+q}}}\right)\left(1-\frac{\varepsilon^-_{\mathbf{k}}\varepsilon^-_{\mathbf{k+q}}+W_{\mathbf{k}}W_{\mathbf{k+q}}}{\sqrt{\left(\varepsilon^-_{\mathbf{k}}\right)^2+W^2_{\mathbf{k}}}\sqrt{\left(\varepsilon^-_{\mathbf{k+q}}\right)^2+W^2_{\mathbf{k+q}}}}\right)\\ &\times\left(\frac{1-f(\Omega^-_{\mathbf{k+q}})-f(\Omega^+_{\mathbf{k}})}{\omega+\Omega^+_{\mathbf{k}}+\Omega^-_{\mathbf{k+q}}+i\delta}+\frac{f(\Omega^+_{\mathbf{k}})+f(\Omega^-_{\mathbf{k+q}})-1}{\omega-\Omega^-_{\mathbf{k+q}}-\Omega^+_{\mathbf{k}}+i\delta}\right)\end{aligned} \tag{A5}$$

$$\begin{aligned}\chi^{(5)}(\mathbf{q},\omega) &= \frac{1}{32}\sum_{\mathbf{k}}\left(1-\frac{E^-_{\mathbf{k}}E^-_{\mathbf{k+q}}+\Delta_{\mathbf{k}}\Delta_{\mathbf{k+q}}}{\Omega^-_{\mathbf{k}}\Omega^-_{\mathbf{k+q}}}\right)\times\left(1+\frac{\varepsilon^-_{\mathbf{k}}\varepsilon^-_{\mathbf{k+q}}+W_{\mathbf{k}}W_{\mathbf{k+q}}}{\sqrt{\left(\varepsilon^-_{\mathbf{k}}\right)^2+W^2_{\mathbf{k}}}\sqrt{\left(\varepsilon^-_{\mathbf{k+q}}\right)^2+W^2_{\mathbf{k+q}}}}\right)\\ &\times\left(\frac{1-f(\Omega^-_{\mathbf{k+q}})-f(\Omega^-_{\mathbf{k}})}{\omega+\Omega^-_{\mathbf{k}}+\Omega^-_{\mathbf{k+q}}+i\delta}+\frac{f(\Omega^-_{\mathbf{k}})+f(\Omega^-_{\mathbf{k+q}})-1}{\omega-\Omega^-_{\mathbf{k+q}}-\Omega^-_{\mathbf{k}}+i\delta}\right)\end{aligned} \tag{A6}$$

$$\chi^{(6)}(\mathbf{q},\omega) = \frac{1}{16}\sum_{\mathbf{k}}\left(1+\frac{E^-_{\mathbf{k}}E^-_{\mathbf{k+q}}+\Delta_{\mathbf{k}}\Delta_{\mathbf{k+q}}}{\Omega^-_{\mathbf{k}}\Omega^-_{\mathbf{k+q}}}\right)\left(1+\frac{\varepsilon^-_{\mathbf{k}}\varepsilon^-_{\mathbf{k+q}}+W_{\mathbf{k}}W_{\mathbf{k+q}}}{\sqrt{\left(\varepsilon^-_{\mathbf{k}}\right)^2+W^2_{\mathbf{k}}}\sqrt{\left(\varepsilon^-_{\mathbf{k+q}}\right)^2+W^2_{\mathbf{k+q}}}}\right)\frac{f(\Omega^-_{\mathbf{k+q}})-f(\Omega^-_{\mathbf{k}})}{\omega-\Omega^-_{\mathbf{k+q}}+\Omega^-_{\mathbf{k}}+i\delta}$$

(A7)

[1] T. Timusk and B. Statt, Rep. Prog. Phys. **62**, 61 (1999); M. R. Norman, D. Pines, and C. Kallin, cond-mat/0507031 (unpublished).

[2] P.W. Anderson *et al.*, J. Phys. Condens. Mat. **16**, R755 (2004); D. A. Ivanov, P. A. Lee, and X.-G. Wen, Phys. Rev. Lett. **84**, 3958 (2000); C.M. Varma, Phys. Rev. Lett **83**, 3538 (1999); V. J. Emery, S. A. Kivelson, and O. Zachar, Phys. Rev. B **56**, 6120 (1997); L. Benfatto, S. Caprara, and C. Di Castro; Eur. Phys. Jour. B **17**. 95 (2000); J. Schmalian, D. Pines, and B. Stojkovic, Phys. Rev. Lett. **80**, 3839 (1998); J.R. Engelbrecht, A. Nazarenko, M. Randeria, and E. Dagotto, Phys. Rev. B **57**, 13406 (1998); Q. Chen, I. Kosztin, B. Janko, and K. Levin, Phys. Rev. B **59**, 7083 (1999); S.C. Zhang, Science **275**, 1089 (1997).

[3] S. Chakravarty, R.B. Laughlin, D.K. Morr, and C. Nayak, Phys. Rev. B**63**, 094503 (2001).

[4] S. Tewari, H.-Y. Kee, C. Nayak, and S. Chakravarty, Phys. Rev. B **64**, 224516 (2001).

[5] S. Chakravarty, C. Nayak, S. Tewari, and X. Yang, Phys. Rev. Lett. **89**, 277003 (2002).

[6] M.V. Eremin, I. Eremin, and A. Terzi, Phys. Rev. B **66**, 104524 (2002).

[7] J. Rossat-Mignod, L.P. Regnault, C. Vettier, P. Bourges, P. Burlet, J. Bossy, Physica C **185-189**, 86 (1991).

[8] H.A. Mook, M. Yethiraj, G. Aeppli, T.E. Mason, and T. Armstrong, Phys. Rev. Lett. **70**, 3490 (1993).

[9] H. F. Fong, B. Keimer, P.W. Anderson, D. Reznik, F. Dogan, and I.A. Aksay, Phys. Rev. Lett. **75**, 316 (1995); *ibid.*, Phys. Rev. B **54**, 6708 (1996); H.F. Fong *et al.*, Nature (London) **398**, 588 (1999); S. Pailhes, Y. Sidis, P. Bourges, V. Hinkov, A. Ivanov, C. Ulrich, L.P. Regnault, and B. Keimer, Phys. Rev. Lett. **93**, 167001 (2004).

[10] P. Bourges, L.P. Regnault, Y. Sidis, and C. Vettier, Phys. Rev. B **53**, 876 (1996); H. He *et al.*, Science **295**, 1045 (2002).

[11] See for review P. Bourges, in "The gap Symmetry and Fluctuations in High Temperature Superconductors" edited by J. Bok, G. Deutscher, D. Pavuna and S.A. Wolf (Plenum Press, 1998).

[12] P. Dai, H.A. Mook, S.M. Hayden, G. Aeppli, T.G. Perring, R.D. Hunt, and F. Dogan, Science **284**, 1344 (1999); P. Dai, M. Yethiraj, H.A. Mook, T.B. Lindemer, and F. Dogan, Phys. Rev. Lett. **77**, 5425 (1996).

[13] H.F. Fong, B. Keimer, D.L. Milius, and I.A. Aksay, Phys. Rev. Lett. **78**, 713 (1997); H.F. Fong *et al.*, Phys. Rev. B **61**, 14773 (2000).

[14] S.M. Hayden, H.A. Mook, P. Dai, T.G. Perring, and F. Dogan, Nature (London) **429**, 531 (2004).

[15] C. Stock, W.J.L. Buyers, R.A. Cowley, P.S. Clegg, R. Coldea, C.D. Frost, R. Liang, D. Peets, D. Bonn, W.N. Hardy, and R. J. Birgeneau Phys. Rev. B **71**, 024522 (2005); C. Stock, W.J.L. Buyers, R. Liang, D. Peets, Z. Tun, D. Bonn, W.N. Hardy, and R.J. Birgeneau, Phys. Rev. B **69**, 014502 (2004).

[16] H.F. Fong *et al.* Phys. Rev. Lett. **75**, 316 (1995); D. Z. Liu, Y. Zha, and K. Levin Phys. Rev. Lett. **75**, 4130 (1995); A. J. Millis and H. Monien Phys. Rev. B **54**, 16172 (1996); A. Abanov, and A.V. Chubukov, Phys. Rev. Lett. **83**, 1652 (1999); T. Dahm, D. Manske, and L. Tewordt, Phys. Rev. B **58**, 12454 (1998); J. Brinckmann and P. A. Lee, Phys. Rev. Lett. **82**, 2915 (1999); Y.-J. Kao, Q. Si, and K. Levin, Phys. Rev. B **61**, R11898 (2000); F. Onufrieva and P. Pfeuty, Phys. Rev. B **65**, 054515 (2002); M. Eschrig and M.R. Norman, Phys. Rev. Lett. **89**, 277005 (2002); D. Manske, I. Eremin, and K. H. Bennemann, Phys. Rev. B **63**, 054517 (2001); M.R. Norman, Phys. Rev. B **61**, 14751 (2000); *ibid* **63**, 092509 (2001); A.V. Chubukov, B. Janko and O. Tchernyshov, Phys. Rev. B **63**, 180507(R) (2001); I. Sega, P. Prelovsek, and J. Bonca, Phys. Rev. B **68**, 054524 (2003).

[17] I.Eremin, D.K. Morr, A.V. Chubukov, K. Bennemann, and M.R. Norman, Phys. Rev. Lett. **94**, 147001 (2005).

[18] L. Yin, S. Chakravarty, and P.W. Anderson, Phys. Rev. Lett. **78**, 3559 (1997); E. Demler and S.C. Zhang, Phys. Rev. Lett. **75**, 4126 (1995); D.K. Morr and D. Pines, Phys. Rev. Lett. **81**, 1086 (1998); M. Vojta and T. Ulbricht Phys. Rev. Lett. **93**, 127002 (2004); G. S. Uhrig, K. P. Schmidt, and M. Grüninger Phys. Rev. Lett. **93**, 267003 (2004); G. Seibold and J. Lorenzana Phys. Rev. Lett. **94**, 107006 (2005).

[19] A. Damascelli, Z. Hussain, and Z.-X. Shen, Rev. Mod. Phys. **75**, 473 (2003).

[20] E. Cappelluti and R. Zeyher, Phys. Rev. B **59**, 6475 (1999); I. Eremin and M. Eremin, J. Supercond. **10**, 459 (1997).

[21] B. Dora, K. Maki, and A. Virosztek, Mod. Phys. Lett. **18**, 327 (2004).

[22] S. Chakravarty, Ch. Nayak, and S. Tewari, Phys. Rev. B **68**, 100504(R) (2003).

[23] B. Valenzuela, E.J. Nicol, and J.P. Carbotte, Phys. Rev. B **71**, 134503 (2005).

[24] See, for example, G.D. Mahan, *Many-Particle Physics*, (Plenum Press, New York and London, 1990).

[25] The results for $\mathrm{Im}\chi_0$ were obtained by using the tetrahedron method[26] to evaluate Eq.(6).

[26] G. Lehmann, and M. Taut, Phys. Stat. Solidi B **54**, 469 (1972).

[27] Despite the doubling of the unit cell one finds for the umklapp susceptibility $\chi(\mathbf{q}, \mathbf{Q}, \omega) = 0$ in the DDW state.